Quantum variational solving of the Wheeler-DeWitt equation

Grzegorz Czelusta and Jakub Mielczarek*

Institute of Theoretical Physics, Jagiellonian University, Łojasiewicza 11, 30-348 Cracow, Poland

(Received 22 December 2021; accepted 4 May 2022; published 2 June 2022)

One of the central difficulties in the quantization of the gravitational interactions is that they are described by a set of constraints. The standard strategy for dealing with the problem is the Dirac quantization procedure, which leads to the Wheeler-DeWitt equation. However, solutions to the equation are known only for specific symmetry-reduced systems, including models of quantum cosmology. Novel methods, which enable solving the equation for complex gravitational configurations, are therefore worth seeking. Here, we propose and investigate a new method of solving the Wheeler-DeWitt equation for minisuperspace models (with a finite number of classical degrees of freedom). The approach employs variational quantum algorithms and is possible to implement on quantum computers. For this purpose, the gravitational system is regularized, by performing spherical compactification of the phase space. This makes the system's Hilbert space finite dimensional and allows to use $SU(2)$ variables, which are easy to handle in quantum computing. The validity of the method is examined in the case of the flat de Sitter universe. Both an emulator of a quantum computer and the IBM superconducting quantum computer have been used. The advantages and limitations of the approach are discussed.

DOI: 10.1103/PhysRevD.105.126005

I. INTRODUCTION

The Hamiltonian of general relativity (GR) is a sum of constraints. The constraints are usually grouped into two sets: a single scalar (Hamiltonian) constraint S and a three-component vector constraint V, so that the gravitational Hamiltonian is

$$H[N,\vec{N}] = S[N] + V[\vec{N}] = \int_\Sigma d^3x NC + \int_\Sigma d^3x \vec{N}\cdot\vec{C}, \quad (1)$$

where Σ is a spatial hypersurface. The N and $\vec{N}$ are the lapse function and the shift vector, respectively, which are integrated with the smeared constraints C and $\vec{C}$. In triad formulation of GR, due to additional local gauge symmetry, the two constraints are supplemented by the Gauss constraint. By imposing the constraints on the kinematical phase space $\Gamma_{\rm kin}$, the physical phase space $\Gamma_{\rm phys}$ is obtained. However, due to the complicated form of the constraints (specifically the smeared scalar constraint C), extraction of the physical phase space is, in general, a difficult task.

This difficulty propagates onto the quantum case where the initial kinematical Hilbert space $\mathcal{H}_{\rm kin}$ is a subject of imposing the quantum constraints $\hat{C}$ and $\hat{\vec{C}}$ in order to extract the physical states $|\Psi_{\rm phys}\rangle$, belonging to the physical Hilbert space $\mathcal{H}_{\rm phys} \subseteq \mathcal{H}_{\rm kin}$ (the equality of sets $\mathcal{H}_{\rm phys} = \mathcal{H}_{\rm kin}$ corresponds to the trivial case of vanishing constraints). Here, for simplicity, we assumed that the kinematical Hilbert is separable (e.g., Fock space). However, this is not necessarily the case in quantum gravity. A seminal example is provided by loop quantum gravity (LQG), where the Hilbert space of almost periodic functions (spin networks) is considered [1,2]. In this case an algebraic dual $\mathcal{D}^*$ (space of distributions) of some dense subspace of $\mathcal{D}$ of $\mathcal{H}_{\rm kin}$ is introduced, so that $\mathcal{D} \subset \mathcal{H}_{\rm kin} \subset \mathcal{D}^*$ (the so-called Gel'fand triple). Eventually, $\mathcal{H}_{\rm phys} \subseteq \mathcal{D}^*$ and $\mathcal{H}_{\rm phys} \not\subseteq \mathcal{H}_{\rm kin}$. In what follows, we will restrict our attention to the case of separable kinematical Hilbert space, which is satisfied for regularized minisuperspace models. Worth noticing is also that, in LQG, the Hilbert space $\mathcal{H}^{G,V}_{\rm kin}$, obtained by solving the quantum Gauss and vector constraints, is separable. Therefore, $\mathcal{H}_{\rm phys} \subseteq \mathcal{H}^{G,V}_{\rm kin}$, where $\mathcal{H}_{\rm phys}$ is obtained by solving the quantum scalar constraint. Therefore, our considerations can be referred to the case $\mathcal{H}^{G,V}_{\rm kin}$ as the kinematical space.

There are various strategies for solving quantum constraints. Before we proceed to reviewing the most common of them, let us restrict our considerations to the case of a single quantum constraint $\hat{C}$—the quantum Hamiltonian constraint (scalar constraint). This assumption is to simplify our considerations and make them more transparent. However, extension to the case of multiple constraints is, in principle, possible. Namely, a given method of solving the single constraint has to be applied repeatedly. However, additional technical difficulties may appear due to differences in the nature and functional form of the

*jakub.mielczarek@uj.edu.pl

constraints (such as the problem with the vector/diffeomorphism constraint in LQG [1]). Furthermore, the case with the single constraint $\hat{C}$ corresponds to homogeneous minisuperspace models, which are relevant in (quantum) cosmology.

Perhaps the most common approach to determine $\mathcal{H}_{\text{phys}}$ is provided by the Dirac method of quantizing constrained systems. Here, taking the $\hat{C}$, which is a self-adjoint operator, one is looking for states which are annihilated by the operator, i.e.,

$$\hat{C}|\Psi\rangle = 0, \tag{2}$$

which is satisfied for the states $|\Psi\rangle \in \mathcal{H}_{\text{phys}}$. Equation (2) is the famous Wheeler-DeWitt (WDW) equation. Solutions to the equation, which belong to the kernel of the operator $\hat{C}$, span the Hilbert space, $\mathcal{H}_{\text{phys}} = \ker\ \hat{C}$. The difficulty of the method lies in finding the solution to the WDW equation. The solutions are known, e.g., for certain quantum cosmological models [3,4]. Furthermore, in the general case, the WDW equation is ill defined and must be regularized [5,6].

Extraction of the physical states can alternatively be performed employing the "group averaging" [7] approach, which utilizes the projection operator $\hat{P}$. The $\hat{P}$ is a nonunitary, but self-adjoint ($\hat{P}^\dagger = \hat{P}$) and idempotent ($\hat{P}^2 = \hat{P}$) operator, which for the case of a constraint $\hat{C}$ with a zero eigenvalue takes the following form:

$$\hat{P} = \lim_{T\to\infty} \frac{1}{2T} \int_{-T}^{T} d\tau\, e^{i\tau\hat{C}}. \tag{3}$$

The expression performs Dirac deltalike action on the kinematical states, projecting them onto the physical subspace.

Another widely explored method of finding the physical states is provided by the "reduced phase space" method [8], in which one looks for a solution of the constraints already at the classical level. For gravity, this is perhaps not possible do, in general. However, utility of the approach has been shown for certain minisuperspace models (see, e.g., [9,10]). While the Γ_{phys} is extracted, the algebra of observables is a subject of quantization, leading to the physical Hilbert space $\mathcal{H}_{\text{phys}}$.

The method we are going to study here is based on the observation made in Ref. [11]. Namely, while a Hamiltonian constraint $C \approx 0$ is considered, the configurations satisfying the constraint can be found by identifying ground states of a new Hamiltonian C^2. A possibility of extracting Γ_{phys} for a prototype classical constraint C with the use of adiabatic quantum computing has been discussed in Ref. [11].

Here, we generalize the method to the quantum case and investigate its implementation on a universal quantum computer. The approach, utilizes a variational quantum eigensolver (VQE) [12], which is a hybrid quantum algorithm. The algorithm has been widely discussed in the literature, in particular, in the context of quantum chemistry [13,14]. While our VQE-based method is introduced in a general fashion, which does not depend on the particular form of $\hat{C}$, over the article we will mostly refer to a concrete $\hat{C}$, corresponding to a quantum cosmological model. The VQE will be implemented on both a simulator of a quantum computer (employing PENNY LANE [15] and QISKIT [16] tools) and on an actual superconducting quantum computer provided by IBM [17].

Applying quantum computing methods unavoidably requires dealing with the finite systems—having finite-dimensional Hilbert spaces. Because standard canonical quantization of gravitational systems does not lead to finite-dimensional Hilbert space representation, a suitable regularization has to be applied. There are various approaches to the problem. In particular, in loop quantum gravity, finite-dimensional Hilbert space can be obtained by fixing a spin network state (fixing a graph and spin labels). Another possibility, starting from GR, may be considered as a sequence of the following three steps:

(1) UV regularization, which reduces gravitational field theory to an infinite-dimensional mechanical system (with a countable number of classical degrees of freedom).
(2) IR regularization, which imposes an upper bound on the number of classical degrees of freedom. This leads us to the realm of minisuperspace models.
(3) Cutoff on the Hilbert space. Quantization of minisuperspace models, in general, leads to infinite-dimensional Hilbert spaces. Even while the resulting WDW equation is regular, the Hilbert space itself requires further regularization, to deal with a finite number of quantum degrees of freedom. This can be done, e.g., by introducing cutoff in the Fock space (see, e.g., [18]).

Here, we consider the case where the minisuperspace model is already obtained (independent of the applied method) and only the third step remains to be made. For this purpose, we apply the recently introduced nonlinear field space theory (NFST) [19–22], which provides a systematic procedure of compactifying phase spaces of the standard affine phase spaces. The compactification leads to finite volume of the phase space and, in consequence, finite dimension of the Hilbert space. In case of the spherical compactification of $\mathbb{R}^2$ phase space, the control parameter of the cutoff is the total spin S, associated with the volume of the spherical phase space. In the large spin limit ($S \to \infty$), the standard case with an infinite-dimensional Hilbert space is recovered. Depending on quantum computational resources, the value of S can be fixed such that the corresponding Hilbert space can be represented with an available number of logical qubits.

Additional advantage of the method introduced in this article is that finding physical states employing variational methods gives us an explicit form of the associated operator (i.e., *Ansatz* with determined parameters), which can be used to generate the physical states on a quantum computer. The states can be used for further simulations on a quantum processor. For example, transition amplitudes between the states can be evaluated. On the other hand, when the physical states are found using analytical methods or classical numerics, the difficulty of constructing operator preparing a given state remains.

The organization of the article is as follows. In Sec. II, the method of regularizing the Hamiltonian constraint, employing compactification of the phase space is introduced. The procedure is applied to the case of de Sitter cosmology. Then, in Sec. III, general considerations concerning the VQE applied to solving the Hamiltonian constraint are made. The qubit representation of the Hamiltonian constraint introduced in Sec. II is discussed in Sec. IV. In Sec. V, the problem of determining the fixed spin subspace of the physical Hilbert space is addressed. A quantum method of evaluating gradients in the VQE procedure is presented in Sec. VI. Examples of applying the procedure for the case of spin $s = 1$ is given in Sec. VII and in Sec. VIII for $s = 2$. The computational complexity considerations of the method are made in Sec. IX. The results are summarized in Sec. X.

II. COMPACT PHASE SPACE REGULARIZATION OF DE SITTER MODEL

The initial step toward quantum variational solving of the Wheeler-DeWitt equation is making the system's Hilbert space finite. Actually, there are theoretical arguments for gravitational Hilbert space being locally finite [23]. Some of the approaches of quantum gravity aim to implement this property while performing quantization of gravitational degrees of freedom [24]. Here, we will follow a general procedure of making gravitational Hilbert space finite, which is based on compactification of the phase space. The approach is considered here as a particular, convenient way of performing regularization of a quantum system. However, it may also play a role in formulating quantum theory of gravitational interaction. However, this second possibility is not explored here, and the method is used purely for technical reasons.

Worth adding here is that the method based on compactification of the phase space can be applied for quantum simulations of other field theories. This, in particular, concerns the case of a quantum scalar field [22]. Furthermore, compactification of the phase space has recently been used for the lattice $U(1)$ gauge fields [25]. In this case, the cylindrical $U(1) \times \mathbb{R}$ phase space per link was compactified to $\mathbb{S}^2$, preserving the $U(1)$ symmetry.

A. Compact phase spaces

Let us recall that, for a system with m classical degrees of freedom, dimension of the phase space Γ is $\dim \Gamma = 2m$. Having the symplectic form ω, defined at the phase space (which is a symplectic manifold), the volume of the space is $\mathcal{V} = \int_\Gamma \omega$. Following the Heisenberg uncertainty principle, one can now estimate the number of linearly independent vectors in the corresponding Hilbert space as follows:

$$\dim \mathcal{H} \sim \frac{\mathcal{V}}{(2\pi\hbar)^m}. \tag{4}$$

It should be noted that, because the Heisenberg uncertainty may differ from the standard form while quantum gravitational degrees of freedom are considered, the formula (4) may be a subject of additional modifications. This should, however, not affect the general observation that dimension of the Hilbert space is monotonically dependent on the volume of the system's phase space. In consequence, finiteness of both the Hilbert space and the phase space are equivalent,

$$\dim \mathcal{H} < \infty \Leftrightarrow \mathcal{V} < \infty. \tag{5}$$

This allows us to conclude that, by performing compactification of the phase space, the resulting quantum system will be characterized by a finite Hilbert space. The observation has been recently pushed forward in NFST [19], with the ambition to introduce compact phase space generalizations, not only of mechanical systems, but also field theories. The procedure has been so far been most extensively studied in the case of a scalar field.

For our purpose, let us focus our attention on the case with a finite number of classical degrees of freedom. This applies to the so-called minisuperspace gravitational systems. Having the m classical degrees of freedom, the standard symplectic form (in the Darboux basis) can be written as

$$\omega = \sum_{i=1}^{m} \omega_i = \sum_{i=1}^{m} dp_i \wedge dq_i, \tag{6}$$

which is defined on the $\Gamma = \mathbb{R}^{2m}$ phase space. There are various ways of performing compactification of the phase space.

B. Spherical phase space

A simple and convenient approach is to replace every $\mathbb{R}^2$ subspace [corresponding to a given conjugated pair (q_i, p_i)] with a two-sphere $\mathbb{S}^2$, so that the total phase space, for the system having m classical degrees of freedom, becomes $\Gamma = \mathbb{S}^{2m}$. This replacement is possible because $\mathbb{S}^2$ is a symplectic manifold, and a product of symplectic manifolds is also symplectic.

There are two main advantages of such a choice. First is the fact that $\mathbb{S}^2$ is a phase space of angular momentum (spin), which results in being easy to handle and a

well-understood representation on both the classical and quantum level. Second, a single new parameter S, associated with the volume of the phase space $\mathcal{V} = \int_{\mathbb{S}^2} \omega_{\mathbb{S}^2} = 4\pi S$, provides a natural control parameter of the regularization. The flat (affine) limit is recovered by taking the $S \to \infty$ limit. On the other hand, selecting a given value of S precisely determines dimension of the Hilbert space. This is because quantization of the spherical phase space leads to the condition $S = \hbar s$, where $s = \frac{n}{2}$, and $n \in \mathbb{N}$. For a given quantum number s, the associated Hilbert space $\mathcal{H}_s$ has dimension $\dim \mathcal{H}_s = 2s + 1$, which leads to concrete realization of the relation (4),

$$\dim \mathcal{H}_s = 2s + 1 = \frac{2S}{\hbar} + 1 = \frac{\mathcal{V}}{2\pi\hbar} + 1. \tag{7}$$

A natural symplectic form of the sphere is $\omega_{\mathbb{S}^2} = S \sin\theta d\phi \wedge d\theta$, where $\phi \in (-\pi, \pi]$ and $\theta \in [0, \pi]$ are spherical angles. It has been shown in [26] that, by applying the change of variables $\varphi = \frac{p}{R_1}$ and $\theta = \frac{\pi}{2} + \frac{q}{R_2}$, together with condition $R_1 R_2 = S$, the symplectic form on the two-sphere takes the form

$$\omega = \cos\left(\frac{q}{R_2}\right) dp \wedge dq. \tag{8}$$

The symplectic form reduces to the flat case in the $S \to \infty$ ($R_{1,2} \to \infty$) limit. Therefore, the symplectic form (8) allows us to recover the flat case locally or in the large S approximation (see Fig. 1).

Because variables p and q do not provide a continuous parametrization of the sphere, it is convenient to work with the spin variables. Here, they correspond to the following Cartesian parametrization of the two-sphere,

$$S_x = S \cos\left(\frac{p}{R_1}\right) \cos\left(\frac{q}{R_2}\right), \tag{9}$$

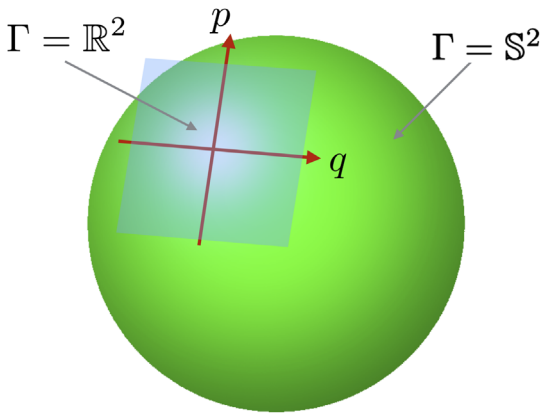

FIG. 1. Illustration of the spherical phase space and its local flat approximation.

$$S_y = S \sin\left(\frac{p}{R_1}\right) \cos\left(\frac{q}{R_2}\right), \tag{10}$$

$$S_z = -S \sin\left(\frac{q}{R_2}\right), \tag{11}$$

together with the condition $S_x^2 + S_y^2 + S_z^2 = S^2$. Employing the symplectic form (8), which defines the Poisson bracket, one can verify that the spin components satisfy the $\mathfrak{su}(2)$ algebra $\{S_i, S_j\} = \epsilon_{ijk} S_k$, where $i, j, k \in \{x, y, z\}$. The algebra is quantized in a straightforward manner, leading to the commutator algebra $[\hat{S}_i, \hat{S}_j] = i\hbar\epsilon_{ijk}\hat{S}_k$. Irreducible representations of the algebra are labeled by the spin s, such that

$$\hat{S}^2 |s, s_z\rangle = \hbar s(s+1) |s, s_z\rangle, \tag{12}$$

$$\hat{S}_z |s, s_z\rangle = \hbar s_z |s, s_z\rangle, \tag{13}$$

where $s_z = -s, -s+1, \ldots, s_1, s$. The eigenstates states $|s, s_z\rangle$ span the Hilbert space for a given representation, i.e., $\mathcal{H}_s = \text{span}\{|s, -s\rangle, \ldots, |s, s\rangle\}$, and $\dim \mathcal{H}_s = 2s + 1$. In what follows, for convenience, we set $\hbar = 1$.

Let us notice that the parametrization (9)–(11) is not a unique choice. In particular, in Ref. [27], polar parametrization of a spherical phase space was considered.

Having defined the spherical compactification procedure at the kinematical level, let us proceed to dynamics. The task is now to replace the flat space variables present in constraints with the spin variables, which are valid for the spherical phase space. It has to be emphasized that the procedure is not unique. However, various assumptions, all satisfying the correspondence to the flat phase space, should converge in the large S limit. A simple choice introduced in [26] is

$$p \to \frac{S_y}{R_2} = R_1 \sin\left(\frac{p}{R_1}\right) \cos\left(\frac{q}{R_2}\right), \tag{14}$$

$$q \to -\frac{S_z}{R_1} = R_2 \sin\left(\frac{q}{R_2}\right), \tag{15}$$

so that the standard case is recovered in the $R_{1,2} \to \infty$ limit. For the system with N degrees of freedom, the same procedure is applied for each (q_i, p_i) pair.

C. De Sitter cosmological model

In this article, we will examine application of the compactification procedure to the flat de Sitter cosmological model (which is a minisuperspace model). The gravitational Hamiltonian constraint for the model can be written as [26]

$$C = q\left(-\frac{3}{4}\kappa p^2 + \frac{\Lambda}{\kappa}\right) \approx 0, \tag{16}$$

where $\kappa := 8\pi G$ and Λ is a positive cosmological constant. Here, the q and p form a canonical pair, for which the symplectic form is $\omega = dp \wedge dq$ (and, in consequence, the canonical Poisson bracket is $\{q, p\} = 1$). The q is related to a cubed scale factor, so that the Hubble factor is $H = \frac{1}{3}\frac{\dot{q}}{q}$. By solving the constraint, the Friedman equation is obtained,

$$H^2 = \frac{\Lambda}{3}. \tag{17}$$

In Ref. [26], a compact phase space generalization of the flat de Sitter cosmological model has been introduced. Following the procedure introduced in the previous subsection, one finds that the compactified form of the constraint (16) is

$$C = \frac{S_3}{R_1}\left[\frac{3}{4}\kappa\frac{S_2^2}{R_2^2} - \frac{\Lambda}{\kappa}\right], \tag{18}$$

where $R_1 R_2 = S$. By introducing the dimensionless parameter

$$\delta := \frac{4}{3}\frac{\Lambda}{R_1^2\kappa^2} \in [0, 1], \tag{19}$$

and by a proper rescaling, the constraint (18) can be rewritten into

$$C \to \frac{4S^2}{3\kappa R_1} C = S_3 S_2^2 - \delta S^2 S_3. \tag{20}$$

Quantization of the constraint (20), which requires promoting of the phase space functions S_x, S_y, and S_z into operators and an appropriate symmetrization, leads to

$$\hat{C} = \frac{1}{3}(\hat{S}_z\hat{S}_y\hat{S}_y + \hat{S}_y\hat{S}_z\hat{S}_y + \hat{S}_y\hat{S}_y\hat{S}_z) - \delta\hat{S}^2\hat{S}_z. \tag{21}$$

It has been shown in Ref. [26] that solutions to the WDW equation associated with the constraint (21) can be found. The solutions are, however, not in a direct form but are expressed in terms of a recursive equation. Furthermore, solutions to the WDW equation exist for the bosonic representations (integer s) and, in general, do not exist for the fermionic representations (half-integer s). The first nontrivial solution to the constraint (21) is for $s = 1$, for which the constraint takes the following matrix form:

$$\hat{C} = 2\left(\frac{1}{6} - \delta\right)\begin{pmatrix} 1 & 0 & 0 \\ 0 & 0 & 0 \\ 0 & 0 & -1 \end{pmatrix} = 2\left(\frac{1}{6} - \delta\right)\hat{S}_z. \tag{22}$$

The corresponding solution (excluding the trivial case of $\delta = \frac{1}{6}$) is given by the state

$$|\Psi\rangle = \begin{pmatrix} 0 \\ 1 \\ 0 \end{pmatrix} = |s = 1, s_z = 0\rangle = \frac{1}{\sqrt{2}}(|01\rangle + |10\rangle), \tag{23}$$

where, in the last equality, qubit representation of the state is given. Therefore, for $s = 1$, dimension of the kernel is $\dim\ker\hat{C} = 1$. On the other hand, as discussed in Ref. [26], for $s = 2$ dimension of the kernel depends on the value of δ. Namely, for $\delta \neq \frac{7}{18}$ we have $\dim\ker\hat{C} = 1$ and for $\delta = \frac{7}{18}$ we have $\dim\ker\hat{C} = 3$. Explicit form of the basis states spanning the kernels can be found in Ref. [26].

It is, of course, tempting to compare the states annihilated by the regularized constraint (21) with results of the canonical quantization of the flat de Sitter model. For this purpose, let us first notice that the canonical quantization case is expected to be recovered in the large spin limit ($S \to 0$). Therefore, the considered $s = 1$ state (23) provides only the lowest order approximation to the result of canonical quantization.

The canonical quantization of the Poisson bracket $\{q, p\} = 1$ leads to the commutation relation $[\hat{q}, \hat{p}] = i\hat{I}$, for which the q representation is $\hat{q}|\psi\rangle = q|\psi\rangle$ and $\hat{p}|\psi\rangle = -i\frac{d}{dq}|\psi\rangle$. The wave function in the q representation is $\psi(q) = \langle q|\psi\rangle$, and the inner product $\langle\psi|\phi\rangle := \int_{\mathbb{R}} dq\psi(q)\phi^*(q)$. The canonical quantization of the classical constraint (16) may employ various factor orderings. The following one, $\hat{C} = \hat{q}(-\frac{3}{4}\kappa\hat{p}^2 + \hat{I}\frac{\Lambda}{\kappa})$, is especially convenient (but not necessarily representative). In this case, the WDW equation reduces to the harmonic form $(\frac{d^2}{dq^2} + \omega^2)\Psi(q) = 0$, where $\omega := \frac{2}{\kappa}\sqrt{\frac{\Lambda}{3}}$. The solutions are incoming and outgoing plane waves $\Psi(q) \propto e^{\pm i\omega q}$, which are non-normalizable.

On the other hand, the q representation of the state (23) (where the spin $s = 1$) is a normalized wave function,

$$\Psi(q) = Y_1^0(\theta, \varphi) = \sqrt{\frac{3}{4\pi}}\frac{1}{2i}(e^{iq/R_2} - e^{-iq/R_2}), \tag{24}$$

which is a real superposition of the two plane waves with frequencies $1/R_2 = \frac{\omega}{S\sqrt{\delta}}$, where $q/R_2 \in [-\pi/2, \pi/2]$. Therefore, the solution (24) agrees qualitatively with the predictions of the canonical quantization [even for very small spins ($s = 1$)].

From Eq. (24) one can see that the probability density $|\Psi(q)|^2$ vanishes at $q = 0$. The same boundary condition can be satisfied by the solutions obtained from the canonical quantization, leading to $\Psi(q) \propto \sin(\omega q)$. Nevertheless, in contrast to the regularized case, the obtained wave function is not square integrable.

Further discussion of the semiclassical limit resulting from the model (21) can be found in Ref. [28].

D. Qubit representation

The introduced compactification not only leads to finite-dimensional Hilbert space, but is also suitable for simulations on a quantum computer. Expressing constraint with the use of spin operators gives a natural qubit representation of the constraint. This is because arbitrary spin s can be decomposed into spin-1/2 representations, which are qubits. One needs $n = 2s$ qubits to implement the spin s representation on a quantum register.

Moreover, eigenstates of the spin operator exhibit symmetry, which can be used to simplify *Ansatz* in variational methods. Eigenstates of the $\hat{S}^2$ operator are invariant under transformation changing order of qubits, i.e., for the operator $\hat{\mathcal{P}}$, defined as

$$\hat{\mathcal{P}}|b_1 b_2 \ldots b_n\rangle = |b_n b_{n-1} \ldots b_1\rangle, \tag{25}$$

and if

$$\hat{S}^2|\psi\rangle = s(s+1)|\psi\rangle, \tag{26}$$

we have

$$\hat{\mathcal{P}}|\psi\rangle = |\psi\rangle. \tag{27}$$

One can simplify the variational *Ansatz* by imposing the $\hat{\mathcal{P}}$ symmetry. Using variational methods, we need to express our constraint in terms of unitary operators. These operators also exhibit the symmetry (i.e., $[\hat{C}, \hat{\mathcal{P}}] = 0$), so we can also reduce the number of terms for which the expectation value must be evaluated. Furthermore, utilizing gradient methods to minimize cost function, we can use the parameter shift rule, which can also be optimized according to the symmetry.

III. VARIATIONAL SOLVING OF A CONSTRAINT

Following the Dirac quantization method of constrained systems, our task is to determine the kernel of the operator $\hat{C}$. The kernel will correspond to the physical Hilbert space for the system $\mathcal{H}_{\text{phys}}$ and is spanned by the states $|\psi_0\rangle \in \mathcal{H}_{\text{phys}}$, annihilated by the Hamiltonian constraint, i.e., satisfying the WDW equation,

$$\hat{C}|\psi_0\rangle = 0. \tag{28}$$

For any linear operator $\hat{C}$, the above condition is equivalent to

$$\langle\psi_0|\hat{C}^\dagger\hat{C}|\psi_0\rangle = 0. \tag{29}$$

Moreover, one can prove that

$$\langle\psi|\hat{C}^\dagger\hat{C}|\psi\rangle \geq 0, \tag{30}$$

for all $|\psi\rangle$. In the case of self-adjoint operator $\hat{C}$, the corresponding conditions are

$$\hat{C}|\psi_0\rangle = 0 \Leftrightarrow \langle\psi_0|\hat{C}^2|\psi_0\rangle = 0, \tag{31}$$

$$\langle\psi|\hat{C}^2|\psi\rangle \geq 0. \tag{32}$$

Following the VQE methods, let us now assume that $|\psi(\boldsymbol{\alpha})\rangle$ is a state parametrized by a vector $\boldsymbol{\alpha} = \{\alpha_i\}_{i=1,\ldots,p}$. In order to find $|\psi_0\rangle$, we have to find a minimum of the non-negative cost function $c(\boldsymbol{\alpha})$, which is defined as follows:

$$c(\boldsymbol{\alpha}) \coloneqq \langle\psi(\boldsymbol{\alpha})|\hat{C}^\dagger\hat{C}|\psi(\boldsymbol{\alpha})\rangle. \tag{33}$$

In the case of the self-adjoint operator $\hat{C}$, the cost function takes the form

$$c(\boldsymbol{\alpha}) = \langle\psi(\boldsymbol{\alpha})|\hat{C}^2|\psi(\boldsymbol{\alpha})\rangle. \tag{34}$$

To find the minimum of c, we use some classical minimizing algorithm (on classical a computer), but the value of c, i.e., expectation value of $\hat{C}^\dagger\hat{C}$, is computed using a quantum computer. The algorithm is initialized with some random parameters $\boldsymbol{\alpha}_0$. Then, by evaluating the quantum circuit, we obtain $c(\boldsymbol{\alpha}_i)$, and using the classical algorithm, we find new parameters $\boldsymbol{\alpha}_{i+1}$, which are closer to minimum; we repeat these steps (see Fig. 2). Eventually, the set of values

$$\boldsymbol{\alpha}_{\min} \coloneqq \arg\min_{\boldsymbol{\alpha}} c(\boldsymbol{\alpha}) \tag{35}$$

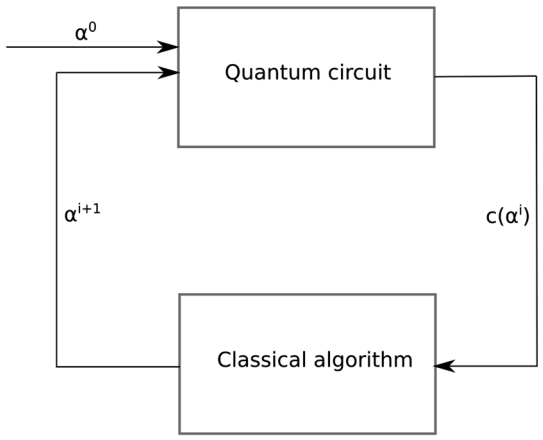

FIG. 2. Schematic illustration of the algorithm of finding the minimum of the cost function, evaluated by a quantum circuit.

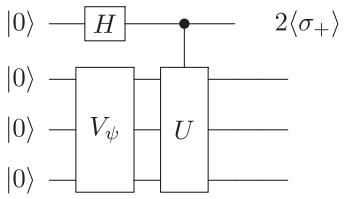

FIG. 3. The Hadamard test—a circuit measuring expectation value of $\hat{U}$ in state $|\psi\rangle$.

is found, such that

$$|\psi_0\rangle = |\psi(\boldsymbol{\alpha}_{\min})\rangle. \tag{36}$$

Because, in general, the kernel space is more that one dimensional, there are different $|\psi_0\rangle$, which satisfy the condition (35). From the perspective of the operator $\hat{C}^\dagger\hat{C}$, this reflects the fact that its ground sate is degenerated. Therefore, the algorithm must be designed such that the whole degeneracy space is sampled.

There are basically two main methods of evaluating the cost function of a quantum computer. The first approach utilizes the so-called Hadamard test and the second follows the method discussed in Ref. [29].

The expectation value of any unitary operator $\hat{U}$ in state $|\psi\rangle$ can be measured using the Hadamard test (Fig. 3), where

$$\hat{V}_\psi|0\rangle = |\psi\rangle. \tag{37}$$

The expectation value of $\hat{U}$ is equal to the expectation value of the operator $2\sigma_+ = \sigma_x + i\sigma_y$ on the first qubit. When $\hat{U}$ is self-adjoint and gives only real expectation values, we can measure just $\langle\sigma_x\rangle$.

In order to compute $\langle 2\sigma_+\rangle = \langle\sigma_x\rangle + i\langle\sigma_y\rangle$, we need to compute $\langle\sigma_x\rangle$ and $\langle\sigma_y\rangle$. For this purpose, we apply a gate, which rotates the base from a computational one to the eigenbasis of a given operator. In the case of $\langle\sigma_x\rangle$, we apply Hadamard operator $\hat{H}$ and take a measurement of σ_z in the computational bases, then

$$\langle\sigma_x\rangle = \langle\hat{H}\sigma_z\hat{H}\rangle = P(0) - P(1). \tag{38}$$

In the case of $\langle\sigma_y\rangle$, we apply operator $\hat{H}\hat{S}^\dagger$, where $\hat{S} = \begin{pmatrix} 1 & 0 \\ 0 & i \end{pmatrix}$ and take a measurement of σ_z in the computational bases, then

$$\langle\sigma_y\rangle = \langle\hat{S}\,\hat{H}\,\sigma_z\hat{H}\hat{S}^\dagger\rangle = P(0) - P(1). \tag{39}$$

Another method of evaluating the expectation value of a unitary operator without additional qubit utilizes the following formula:

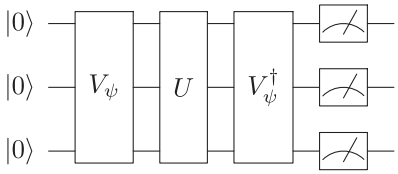

FIG. 4. The circuit measuring expectation value of $\hat{U}$ in state $|\psi\rangle$.

$$\langle\psi|\hat{U}|\psi\rangle = \langle 0|\hat{V}_\psi^\dagger\hat{U}\hat{V}_\psi|0\rangle. \tag{40}$$

So, when we apply the operators V_ψ, U, and $V_\psi^\dagger$ on the initial state $0\rangle$ and measure probability of a state $|0\rangle$ in the final state, we obtain $|\langle\psi|\hat{U}|\psi\rangle|^2$ (see Fig. 4).

In both methods, the $\hat{U}$ is a unitary operator. In the case of nonunitary operators, one has to express the operator as a sum of unitary operators and compute the expectation value of each unitary term separately.

IV. COMPUTING EXPECTATION VALUES

Let us now proceed to the implementation of the algorithm introduced in the previous section. For this purpose, a method of evaluating the mean value of the operator $\hat{C}^2$ has to be introduced.

Our strategy is to express $\hat{C}$ as a sum of tensor products of Pauli operators (for the spin-1/2 representation),

$$\hat{C} = \sum_j c_j \bigotimes_i {}^{\cdot}\hat{\sigma}_{ij}^k, \tag{41}$$

where $k = x, y, z$ indicates one of the Pauli matrices, i is an index of a qubit, and j is an index of a term in the sum. The c_j are constants multiplying a given product of Pauli operators contributing to the sum. Then each part of this sum is a unitary operator and the expectation value can be easily calculated,

$$\langle\hat{C}\rangle = \sum_j c_j \langle\bigotimes_i \hat{\sigma}_{ij}^k\rangle. \tag{42}$$

Here, we apply the method to the constraint (21), which is a function of the spin variables $\hat{S}_i$, corresponding to a spin number s. The operators can be expressed in terms of the Pauli matrices as follows:

$$\hat{S}_i = \frac{1}{2}\sum_{j=1}^{n} \mathbb{I}^1 \otimes \ldots \mathbb{I}^{j-1} \otimes \hat{\sigma}_i^j \otimes \mathbb{I}^{j+1} \otimes \ldots \mathbb{I}^n, \tag{43}$$

where $n = 2s$. It is easy to verify that the spin components $\hat{S}_i$ obey the commutation relation

$$[\hat{S}_i,\hat{S}_j]=\left[\frac{1}{2}\sum_m\hat{\sigma}_i^m,\frac{1}{2}\sum_n\hat{\sigma}_j^n\right]=\frac{1}{4}\sum_{m,n}[\hat{\sigma}_i^m,\hat{\sigma}_j^n]$$
$$=\frac{1}{4}\sum_n[\hat{\sigma}_i^n,\hat{\sigma}_j^n]=\frac{1}{2}\sum_n i\epsilon_{ijk}\hat{\sigma}_k^n$$
$$=i\epsilon_{ijk}\hat{S}_k, \tag{44}$$

where the condition

$$[\hat{\sigma}_i^m,\hat{\sigma}_j^n]=0 \tag{45}$$

for $m\neq n$ has been used. For convenience, we also define

$$P_n(\sigma_i)\coloneqq\sum_j\mathbb{I}^1\otimes\ldots\mathbb{I}^{j-1}\otimes\sigma_i^j\otimes\mathbb{I}^{j+1}\otimes\ldots\mathbb{I}^n, \tag{46}$$

$$P_n(\sigma_i,\sigma_j)\coloneqq\sum_{k,l,k\neq l}\mathbb{I}^1\otimes\ldots\mathbb{I}^{k-1}\otimes\sigma_i^k\otimes\mathbb{I}^{k+1}\otimes\ldots\mathbb{I}^{l-1}$$
$$\otimes\sigma_j^l\otimes\mathbb{I}^{l+1}\otimes\ldots\mathbb{I}^n, \tag{47}$$

$$P_n(\sigma_i,\sigma_j,\sigma_p)\coloneqq\sum_{k,l,q,k\neq l,k\neq q,l\neq q}\mathbb{I}^1\otimes\ldots\sigma_i^k\otimes\ldots\sigma_j^l$$
$$\otimes\ldots\sigma_p^q\otimes\ldots\mathbb{I}^n, \tag{48}$$

so that we can express

$$\hat{S}_i=\frac{1}{2}P_n(\sigma_i), \tag{49}$$

$$\hat{S}_i\hat{S}_j=\frac{1}{4}(P_n(\sigma_i,\sigma_j)+i\epsilon_{ijk}P_n(\sigma_k)+n\delta_{ij}\mathbb{I}^{\otimes n}), \tag{50}$$

$$8\hat{S}_i\hat{S}_j\hat{S}_l=P_n(\sigma_i,\sigma_j,\sigma_l)+i\epsilon_{ilk}P_n(\sigma_k,\sigma_j),$$
$$+i\epsilon_{jlk}P_n(\sigma_k,\sigma_i)+i\epsilon_{ijk}P_n(\sigma_k,\sigma_l)$$
$$+\delta_{il}(n-1)P_n(\sigma_j)+\delta_{jl}(n-1)P_n(\sigma_i)$$
$$-\epsilon_{ijk}\epsilon_{klm}P_n(\sigma_m)+\delta_{ij}nP_n(\sigma_l)+i\epsilon_{ijl}n\mathbb{I}^{\otimes n}. \tag{51}$$

Applying these expressions to Eq. (21), we find that

$$\hat{C}=\frac{1}{8}\Bigg((1-\delta)P_n(\sigma_z,\sigma_y,\sigma_y)-\delta P_n(\sigma_z,\sigma_x,\sigma_x)$$
$$-\delta P_n(\sigma_z,\sigma_z,\sigma_z)+\left(n-\frac{2}{3}-\delta(5n-2)\right)P_n(\sigma_z)\Bigg). \tag{52}$$

For the purpose of constructing the cost function, the square of the operator $\hat{C}$ has to be evaluated. Employing methods of symbolic algebra, the expression for $\hat{C}^2$ can be found explicitly,

$$\hat{C}^2=\frac{1}{64}\Bigg(P_n(\sigma_y,\sigma_y,\sigma_y,\sigma_y,\sigma_z,\sigma_z)(1-\delta)^2+P_n(\sigma_y,\sigma_y,\sigma_y,\sigma_y)(n-4)(1-\delta)^2+P_n(\sigma_y,\sigma_y,\sigma_z,\sigma_z)$$
$$\times\left(4(n-4)(1-\delta)^2-8\delta(1-\delta)-6(n-4)\delta(1-\delta)-12\delta^2+2\left(\frac{3n-2}{3}-\delta(5n-2)\right)(1-\delta)\right)+P_n(\sigma_y,\sigma_y)$$
$$\times\left(4(n-2)(n-3)(1-\delta)^2-8(n-2)\delta^2+2(n-2)\left(\frac{3n-2}{3}-\delta(5n-2)\right)(1-\delta)\right)+P_n(\sigma_z,\sigma_z)(2(n-2)(n-3)$$
$$\times(1-\delta)^2+20(n-2)(n-3)\delta^2+\left(\frac{3n-2}{3}-\delta(5n-2)\right)^2+4(n-2)\delta(1-\delta)-6(n-2)\left(\frac{3n-2}{3}-\delta(5n-2)\right)\delta)$$
$$+\mathbb{I}^{\otimes n}\left(2n(n-1)(n-2)(1-\delta)^2+8n(n-1)(n-2)\delta^2+n\left(\frac{3n-2}{3}-\delta(5n-2)\right)^2\right)+P_n(\sigma_x,\sigma_x)$$
$$\times\left(4(n-2)(1-\delta)^2+4(n-2)(n-3)\delta^2+12(n-2)\delta(1-\delta)-2(n-2)\left(\frac{3n-2}{3}-\delta(5n-2)\right)\delta\right)$$
$$+P_n(\sigma_x,\sigma_x,\sigma_x,\sigma_x,\sigma_z,\sigma_z)\delta^2+P_n(\sigma_x,\sigma_x,\sigma_x,\sigma_x)(n-4)\delta^2+P_n(\sigma_x,\sigma_x,\sigma_z,\sigma_z)\Bigg(10(n-4)\delta^2-8\delta(1-\delta)$$
$$-2\left(\frac{3n-2}{3}-\delta(5n-2)\right)\delta+12\delta(1-\delta)\Bigg)+P_n(\sigma_z,\sigma_z,\sigma_z,\sigma_z,\sigma_z,\sigma_z)\delta^2-2P_n(\sigma_x,\sigma_x,\sigma_y,\sigma_y,\sigma_z,\sigma_z)\delta(1-\delta)$$
$$+P_n(\sigma_z,\sigma_z,\sigma_z,\sigma_z)\left(9(n-4)\delta^2-2\left(\frac{3n-2}{3}-\delta(5n-2)\right)\delta+4\delta(1-\delta)\right)+P_n(\sigma_x,\sigma_x,\sigma_y,\sigma_y)(-2\delta(1-\delta)(n-4)$$
$$+2(1-\delta)^2+4\delta^2+8\delta(1-\delta))-2P_n(\sigma_y,\sigma_y,\sigma_z,\sigma_z,\sigma_z,\sigma_z)\delta(1-\delta)+2P_n(\sigma_x,\sigma_x,\sigma_z,\sigma_z,\sigma_z,\sigma_z)\delta^2\Bigg). \tag{53}$$

V. FIXED SPIN SUBSPACE OF A QUANTUM REGISTER

In order to find the kernel of $\hat{C}$ we have to generate states $|\psi(\boldsymbol{\alpha})\rangle$. In case of two qubits, we can use circuits allowing us to generate any state, but in the case of the arbitrary many qubits there are no such algorithms and we have to use some *Ansatz*, for example, R_y or R_yR_z *Ansatz*. Furthermore, often we want to look for the states only in some subspace of all possible n-qubit states. This is the case in the model under consideration, for which the constraint (21) is defined in the spin-s subspace of the quantum register of n-qubits. One possible approach to this issue is generating only states obeying a given condition. The possibility is, however, difficult to implement in general. Another solution is to generate arbitrary states of the n-qubit register and add a second term to the cost function, which fixes a given spin-s subspace.

Let us consider selection of a subspace, which is an eigenspace of some operator $\hat{D}$,

$$\hat{D}|\psi_d\rangle = d|\psi_d\rangle. \tag{54}$$

Then, we have to extend the cost function by adding a term that has minimum value (equal 0) for states from this subspace, i.e.,

$$\langle\psi|(\hat{D}-d\mathbb{I})^\dagger(\hat{D}-d\mathbb{I})|\psi\rangle = \langle\hat{D}^\dagger\hat{D}\rangle_\psi - 2\Re(d\langle\hat{D}^\dagger\rangle_\psi) + |d|^2. \tag{55}$$

In consequence, the new cost function takes the form

$$c(\boldsymbol{\alpha}) = \langle\psi(\boldsymbol{\alpha})|\hat{C}^\dagger\hat{C}|\psi(\boldsymbol{\alpha})\rangle + \langle\psi(\boldsymbol{\alpha})|(\hat{D}-d\mathbb{I})^\dagger(\hat{D}-d\mathbb{I})|\psi(\boldsymbol{\alpha})\rangle. \tag{56}$$

Because of the numerical minimization issues, it is, however, better to consider a normalized cost function. In our case, we normalized both terms individually, so the normalized first term is equal,

$$\frac{1}{\max|\lambda_i|^2}\langle\psi(\boldsymbol{\alpha})|\hat{C}^\dagger\hat{C}|\psi(\boldsymbol{\alpha})\rangle, \tag{57}$$

where $\max|\lambda_i|^2$ is the modulus square of the biggest eigenvalue of $\hat{C}$. The normalized second term is

$$\frac{1}{\max|d_i-d|^2}\langle\psi(\boldsymbol{\alpha})|(\hat{D}-d\mathbb{I})^\dagger(\hat{D}-d\mathbb{I})|\psi(\boldsymbol{\alpha})\rangle, \tag{58}$$

where d_i are eigenvalues of $\hat{D}$.

In case we *a priori* do not know these eigenvalues, we can treat them as some parameter that has to be adjusted during simulation, or we can try to maximize the cost function and in this way estimate the value of $\max|\lambda_i|^2$. At the end, we normalize both terms dividing them by two (we also can take these two terms with some weights different than $\frac{1}{2}$ in order to improve performance of algorithms in some cases). In this way, the cost function takes values from the interval [0, 1],

$$0 \le c(\boldsymbol{\alpha}) \le 1. \tag{59}$$

In case of the constraint (21), we want to look for a kernel in the subspace of a given spin s. Therefore, we need to take the cost function with $\hat{D} = \hat{\vec{S}}^2 = \hat{D}^\dagger$ and $d = s(s+1)$. However, in this case, we can choose a simpler second term of the cost function,

$$s(s+1) - \langle\hat{\vec{S}}^2\rangle, \tag{60}$$

which after normalization is

$$1 - \frac{\langle\hat{\vec{S}}^2\rangle}{s(s+1)}. \tag{61}$$

Because (assuming that we use only $n = 2s$ qubits) the operator $\vec{S}^2$ has maximal expectation value equal to $s(s+1)$ and minimal equal 0, so

$$0 \le 1 - \frac{\langle\vec{S}^2\rangle}{s(s+1)} \le 1. \tag{62}$$

The zero value corresponds only to the states with spin s. So the whole cost function has zero value only for states that are simultaneously in the kernel of $\hat{C}$ and have spin s. As a spin operator can be expressed in terms of qubits, employing Eq. (49), we find that

$$\vec{S}^2 = \sum_{i=x,y,z} S_i^2 = \frac{3}{4}n\mathbb{I}^{\otimes n} + \frac{1}{4}P_n(\sigma_x,\sigma_x) + \frac{1}{4}P_n(\sigma_y,\sigma_y) + \frac{1}{4}P_n(\sigma_z,\sigma_z), \tag{63}$$

and, consequently,

$$\langle\vec{S}^2\rangle = \frac{3}{4}n + \frac{1}{4}\langle P_n(\sigma_x,\sigma_x)\rangle + \frac{1}{4}\langle P_n(\sigma_y,\sigma_y)\rangle + \frac{1}{4}\langle P_n(\sigma_z,\sigma_z)\rangle. \tag{64}$$

A. Degenerate kernel

In the case of the degenerate kernel (i.e., there are more than one eigenstate for eigenvalue 0), we have to first find some eigenstate $|\psi_1\rangle$ using the presented cost function and then, in order to find another eigenstate (orthogonal to the first one), we have to add to the cost function the following term:

$$|\langle\psi_1|\psi(\boldsymbol{\alpha})\rangle|. \tag{65}$$

This term can easily be evaluated using $\langle 0|\hat{V}_{\psi_1}\hat{V}^{\dagger}_{\psi(\boldsymbol{\alpha})}|0\rangle$, where $\hat{V}_{\psi}$ generates state $|\psi\rangle$. Using this new cost function, we can find another state from kernel $|\psi_2\rangle$ and then, adding to the cost function the new term

$$|\langle\psi_2|\psi(\boldsymbol{\alpha})\rangle|, \tag{66}$$

we can find the third state, and so on.

Another method is to find different vectors from the kernel using an algorithm starting from different initial parameters and then orthogonalize these vectors using the Gram-Schmidt procedure. When Gram-Schmidt returns a zero vector that means that we reached dimension of the kernel (or that we generated a linearly dependent vector so we have to repeat the procedure to have a high level of confidence that there are no more linearly independent vectors in kernel subspace).

VI. GRADIENT METHODS

In order to find the minimum of cost function, one needs to use some classical optimizer. There are possible choices of optimizers that do not need gradient of cost function, for example, the COBYLA optimizer [30]. But one can get better performance using a gradient descent optimizer, for example, a basic gradient descent optimizer that in each step computes the new values according to the rule

$$x^{(t+1)} = x^{(t)} - \eta\nabla f(x^{(t)}). \tag{67}$$

Another possibility includes more sophisticated algorithms like the Adam optimizer [31]. Using a gradient method, one needs to compute the gradient of a cost function. One way to do so is to calculate values of the cost function in two points and compute the numerical derivative by finite differences. Another way is to use the parameter-shift rule [32]. Let us consider function f, which is an expectation value of some operator $\hat{U}$ in some, parametrized by θ, state $|\psi(\theta)\rangle = \hat{V}_{\theta}|0\rangle$,

$$f(\theta) = \langle U\rangle_{\psi_\theta} = \langle 0V^{\dagger}_{\theta}UV_{\theta}0\rangle \tag{68}$$

and assume that V_θ can be factorized (i.e., in circuit representing V_θ there is 1-qubit gate G_{θ_i}),

$$V_\theta = A_{\theta_0,\ldots,\theta_i-1}G_{\theta_i}B_{\theta_i+1,\ldots,\theta_n}, \tag{69}$$

where

$$G_{\theta_i} = e^{-i\theta_i\mathcal{G}}, \tag{70}$$

and $\mathcal{G}$ is a self-adjoint operator with two different eigenvalues $-r, +r$. Then, the exact (not approximate) derivative of f with respect to θ_i is

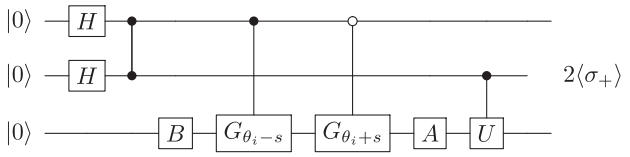

FIG. 5. A quantum circuit corresponding to the parameter-shift rule in the case of 1-qubit states and operators.

$$\partial_{\theta_i}f = r(f(\theta_i + s) - f(\theta_i - s)), \tag{71}$$

where $s = \frac{\pi}{4r}$. In frequent cases of rotations around Pauli matrices (as in popular *Ansätze*), $G = R_y, R_x, R_z$, parameter r equals 1. Evaluation of a difference between shifted functions can be made with the use of the circuit shown in Fig. 5. Then, the expectation value of $2\langle\sigma_+\rangle$ is equal to the derivative of f,

$$2\langle\sigma_+\rangle = f(\theta_i + s) - f(\theta_i - s) = \partial_{\theta_i}f. \tag{72}$$

VII. THE $s = 1$ CASE

As the first example of the introduced method, let us consider the special case of $s = 1$, for which the constraint takes the form

$$\hat{C} = \left(\frac{1}{6} - \delta\right)P_n(\sigma_z) = \left(\frac{1}{6} - \delta\right)(\sigma_z \otimes \mathbb{I} + \mathbb{I} \otimes \sigma_z), \tag{73}$$

and its square

$$\hat{C}^2 = 2\left(\frac{1}{6} - \delta\right)^2(\mathbb{I} \otimes \mathbb{I} + \sigma_z \otimes \sigma_z). \tag{74}$$

Therefore, we need to compute only one expectation value,

$$\langle\hat{C}^2\rangle = 2\left(\frac{1}{6} - \delta\right)^2(1 + \langle\sigma_z \otimes \sigma_z\rangle). \tag{75}$$

The quantum circuit enabling measuring the expectation value $\langle\sigma_z \otimes \sigma_z\rangle$ is shown in Fig. 6.

As the $\hat{V}_\psi$ operator we use the RYCZ *Ansatz* with two angles $\theta_1, \theta_2 \in [0, 2\pi)$ (see the Appendix). The quantum circuit for the *Ansatz* is shown in Fig. 7. We reduced the number of parameters from 4 to 2 using symmetry of our constraint, which induces symmetry of states from the

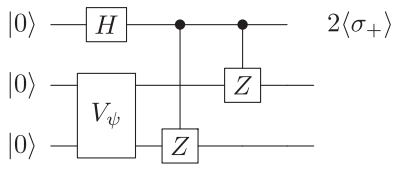

FIG. 6. A quantum circuit measuring expectation value $\langle\sigma_z \otimes \sigma_z\rangle$ in state $|\psi\rangle$.

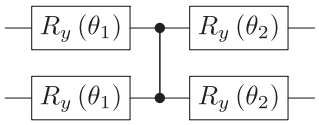

FIG. 7. A quantum circuit for the *Ansatz* for the spin-1 case.

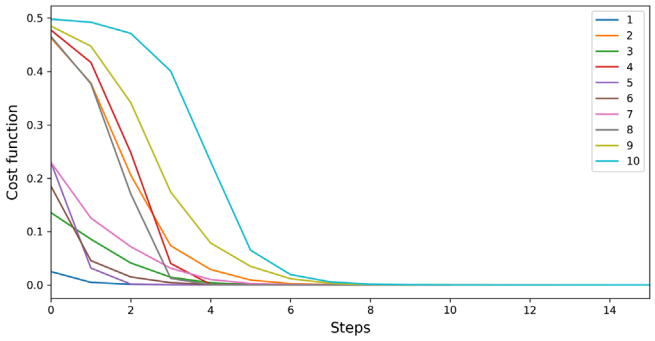

FIG. 8. Evolution of the cost function during minimization, for ten runs with randomly initialized parameters.

kernel. The states are, namely, invariant under changing qubits order from $q_1, q_2, \ldots, q_n$ to $q_n, q_{n-1}, \ldots, q_1$.

In this example, a basic gradient descent optimizer was used with step size $\eta = 1$ and convergence tolerance was 10^{-6}. Parameter δ in the constraint was set to $\frac{1}{2}$.

Figure 8 shows the cost function in a function of steps of the optimization procedure.

Figure 9 shows the cost function in the parameter space. We see four minima, each corresponding to the same state (up to a global phase). It is worth noticing that the landscape of the cost function does not possess any local minima, which simplifies the optimization procedure. This, however, is not necessarily the case for higher spins, including the spin-2 example discussed in the next section.

Obtained amplitudes of the basis states are shown later. The algorithm returns correct states up to the global sign (in

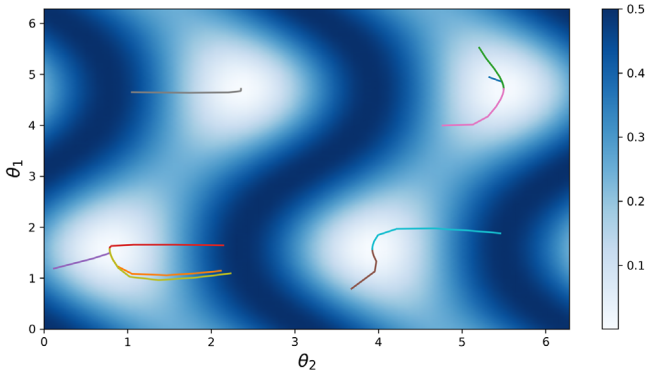

FIG. 9. Parameters of states for each step in the space of all possible parameters for the case of a quantum simulator. The colors of the curves correspond to those in Fig. 8. The heat map represents value of the cost function.

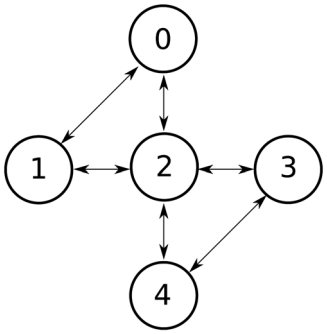

FIG. 10. Connectivity of qubits in the Yorktown processor.

what follows the signs are agreed). The states are very close to the exact result, which is a state $\frac{1}{\sqrt{2}}(|01\rangle + |10\rangle)$ [see Eq. (23)], with quantum fidelity equal 1, up to numerical uncertainty. Because the RYCZ *Ansatz* corresponds to a pure state, the quantum fidelity reduces to $F(\hat{\rho}_1, \hat{\rho}_2) = |\langle\psi_1|\psi_2\rangle|^2$, where $\hat{\rho}_1 = |\psi_1\rangle\langle\psi_1|$ and $\hat{\rho}_2 = |\psi_2\rangle\langle\psi_2|$.

For this simple case, we also did computation on the real IBM superconducting quantum processor Yorktown [17]. The quantum processor has a topology of qubits as shown in Fig. 10. In the simulations, 1024 of shots for each circuit were made.

Figure 11 shows the cost function in a function of steps of the optimization procedure.

Figure 12 shows the cost function in the parameter space.

In consequence of the applied optimization procedure, the state, for which measured amplitudes are shown in Fig. 13, has been found. Without error correction methods and with automatic transpilation of circuit, we obtained fidelity of the found state equal 0.9973 ± 0.0029.

VIII. THE $s = 2$ CASE

In this case, the constraint squared consists of more Pauli terms, which have to be evaluated independently and then summed up,

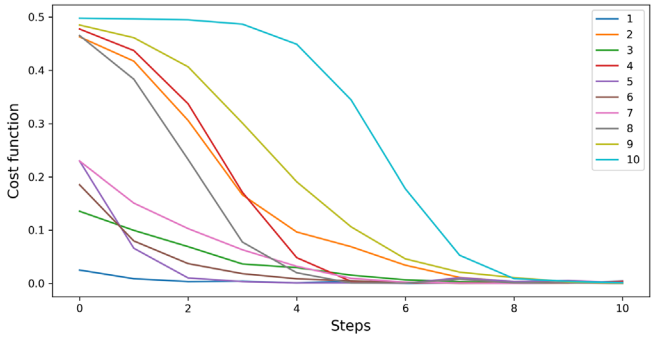

FIG. 11. Evolution of the cost function during minimization, for ten runs with randomly initialized parameters. Values computed on simulator based on parameters obtained on the IBM Yorktown quantum computer.

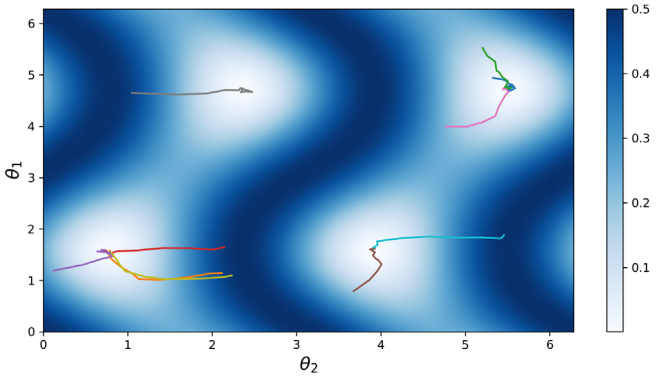

FIG. 12. Parameters of states for each step in the space of all possible parameters for the case of the Yorktown quantum processor. The colors of the curves correspond to those in Fig. 11. The heat map represents values of the cost function.

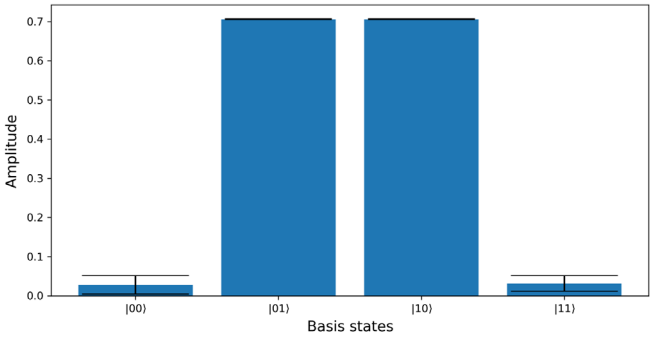

FIG. 13. Averaged (over ten runs) amplitudes of the final state. Here, the RYCZ *Ansatz* implies that the amplitudes are real valued. The error bars correspond to standard deviation.

$$\hat{C}^2 = \frac{1}{16}\left(P_n(\sigma_y,\sigma_y)\left(\frac{16}{3}-\frac{76}{3}\delta+16\delta^2\right)+P_n(\sigma_z,\sigma_z)\right.$$
$$\times\left(\frac{34}{9}-40\delta+144\delta^2\right)+P_n(\sigma_x,\sigma_x)\left(2-\frac{4}{3}\delta+16\delta^2\right)$$
$$+\mathbb{I}^{\otimes 4}\left(\frac{208}{9}-144\delta+384\delta^2\right)+P_n(\sigma_x,\sigma_x,\sigma_y,\sigma_y)$$
$$+P_n(\sigma_z,\sigma_z,\sigma_z,\sigma_z)\left(-\frac{2}{3}\delta+8\delta^2\right)+P_n(\sigma_y,\sigma_y,\sigma_z,\sigma_z)$$
$$\left.\times\left(\frac{5}{3}-\frac{38}{3}\delta+8\delta^2\right)+P_n(\sigma_x,\sigma_x,\sigma_z,\sigma_z)\left(-\frac{2}{3}\delta+8\delta^2\right)\right). \tag{76}$$

Here, we use also the RYCZ *Ansatz* but for four qubits, with two layers and six real parameters (see Fig. 14).

Figure 15 shows the cost function in a function of steps of the optimization procedure employing the simulator of a quantum computer.

In all cases (six out of ten) when the cost function decreases under 0.004, we obtain states with fidelity above 0.98, in cases (two out of ten) with the cost function slightly above 0.04, we obtain fidelity around 0.64. Interesting is the case with high fidelity 0.93, but with cost function quite high 0.009, which means that even if we stuck in some local minimum, we have a chance to obtain a state close to the correct one. The obtained fidelities are collected in Table I.

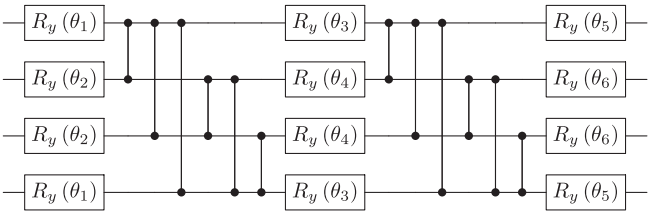

FIG. 14. Quantum circuit for the *Ansatz* for spin 2.

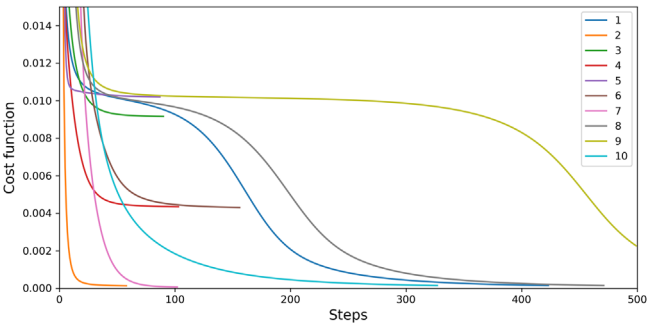

FIG. 15. Cost function during minimization for ten runs with randomly initialized parameters. Here, the RYCZ *Ansatz* and $\delta = 1/2$ have been used.

In the case of $s = 2$ for $\delta = \frac{7}{18}$ the kernel of $\hat{C}$ is degenerated, $\dim\ker\hat{C} = 3$. A linearly independent set of states spanning the kernel can be found using the method discussed in Sec. V. In this case, we define fidelity of the found states in the following way:

$$F(\psi,\phi_1,\phi_2,\phi_3) := |\langle\psi|\phi_1\rangle|^2 + |\langle\psi|\phi_2\rangle|^2 + |\langle\psi|\phi_3\rangle|^2. \tag{77}$$

TABLE I. Fidelities of the obtained states and final values of the cost function corresponding to these states for ten runs.

No.	Fidelity	Cost
1	0.99825	0.00014
2	0.99831	0.00013
3	0.92892	0.00915
4	0.63477	0.00434
5	0.00383	0.01019
6	0.64508	0.00430
7	0.99777	0.00006
8	0.99825	0.00014
9	0.98189	0.00226
10	0.99825	0.00014

TABLE II. Fidelity (77) of each state obtained for five runs of the optimization procedure for the case with $s = 2$ and $\delta = \frac{7}{18}$.

No.	State 1	State 2	State 3	State 4
0	0.99982	0.99984	0.99991	0.99989
1	0.99984	0.99999	0.99989	0.99993
2	0.99992	0.99995	0.99989	0.99983
3	0.99984	0.99988	0.99985	0.99995
4	0.99984	0.99990	0.99985	0.99999

TABLE III. Norms of states obtained in each step of the Gram-Schmidt procedure (before normalization of the sates) for five runs of the optimization procedure for the case with $s = 2$ and $\delta = \frac{7}{18}$.

No.	Step 1	Step 2	Step 3	Step 4
1	1.0000	0.9998	0.0764	0.0006
2	1.0000	0.9038	0.6065	0.0002
3	1.0000	0.1097	0.4148	0.0040
4	1.0000	0.9984	0.0003	0.2669
5	1.0000	0.7227	0.0000	0.8264

Here, $|\psi\rangle$ is the determined state and $|\phi_i\rangle$ are the exact states forming an orthonormal basis in the kernel subspace. In Table II, fidelities of the obtained states are shown. The results of the Gram-Schmidt procedure for five runs are collected in Table III. In all case, there are three leading contributions and the fourth one is marginal. This provides evidence that the kernel space is three dimensional, in accordance with the theoretical expectations for the case with $\delta = \frac{7}{18}$. However, due to computational errors, the answer is not fully conclusive.

IX. COMPUTATIONAL COMPLEXITY

As we see, the case $s = 2$ has many more terms to evaluate than the case $s = 1$. Consequently, in the large spin limit, a problem of an enormous number of terms may arise. To analyze the number of Pauli terms for arbitrary spin s, let us first notice that the number of different Pauli terms in operator P_n is given by the combinatorial factor

$$\frac{n!}{n_x!n_y!n_z!(n-n_x-n_y-n_z)!}, \tag{78}$$

where n_k is the number of Pauli operators σ^k, and n is the number of qubits. Using formula (53) for C^2 for arbitrary spin, we obtain (for $n \geq 6$) a number of Pauli terms, i.e., number of quantum circuits to evaluate is

$$\frac{151}{720}n(n-1)(n-2)(n-3)(n-4)(n-5) + \frac{7}{8}n(n-1)(n-2)(n-3) + \frac{3}{2}n(n-1) \sim n^6, \tag{79}$$

which, fortunately, has polynomial computational complexity $\mathcal{O}(n^6)$. Here, symmetries of the constraint (which may slightly reduce the number of combinations) were not taken into account.

Another aspect of computational complexity of the method relates to the fact that in the proposed method a subspace of the total Hilbert space of the quantum register is used. For a register composed of n qubits, the Hilbert space has dimension 2^n. However, the constraint (with fixed spin s) subspace forms a $2s + 1 = n + 1$-dimensional subspace. The remaining $2^n - (n + 1)$ states of the register are not used. This is unavoidably a waste of quantum resources and the weak side of the approach. Please notice that the spin s scales linearly with the number of qubits. So, for instance, with 16 qubits we can simulate only a system with spin $s = 8$.

The ideal situation would be to utilize the whole Hilbert space of the quantum register, so that $2s + 1 = 2^n$. In such case, having $n = 16$ qubits allows one to simulate with $s \sim 3 \times 10^4$. Finding a method of representing spin operators and constraints in this case is an open problem, which will be addressed elsewhere.

It should be noted that, in principle, we can always express our constraints, considered as a matrices, in terms of Pauli strings acting on all qubits, so that the number of qubits is $n = \lceil \log_2(2s + 1) \rceil$. However, it is generally difficult to find this decomposition, and our approach is easier to implement and generalize. For example, Eq. (53) gives this expansion of our constraint for arbitrary spin.

The advantage of the method presented here becomes, however, sound, while systems with sufficiently high numbers (m) of the classical degrees of freedom are considered. Then, assuming that for every degree of freedom the spin representation is s, the dimension of the Hilbert space of the composite system is $(2s + 1)^m$. Every spin consumes $n = 2s$ qubits of the quantum register, so in total $nm = 2sm$ qubits are needed. So, the smaller the s, the less of the quantum resources are wasted, i.e., $2^{2sm} - (2s + 1)^m$. In the limiting case of $s = 1/2$, all the quantum resources are utilized $2^{2\frac{1}{2}m} - (2\frac{1}{2} + 1)^m = 0$. In this range, application of quantum methods promises to be advantageous over the classical method, since the amount of utilized computational resources grows exponentially with m.

X. SUMMARY

In this article, we have introduced and tested a method of solving of the minisuperspace Wheeler-DeWitt equation employing variational quantum methods. For a single constraint C, with m classical degrees of freedom, the methods consist of the following main steps:

(1) Replace the kinematical phase space $\Gamma = \mathbb{R}^{2m}$ with $\Gamma = \mathbb{S}^{2m}$.

(2) Express the constraint C in terms of spin variables $C(\vec{S}_1, \ldots, \vec{S}_m)$. This can be done by applying the replacement

$$p \to \frac{S_y}{R_2}, \qquad q \to -\frac{S_z}{R_1},$$

where $R_1 R_2 = S$, for every canonical pair (q_i, p_i).

(3) Perform canonical quantization and symmetrization of the constraint, obtaining $\hat{C}(\hat{\vec{S}}_1, \ldots, \hat{\vec{S}}_m)$. Fix a particular representation s for the spins.

(4) Represent the spin operators in terms of qubits, employing the formula

$$\hat{S}_i = \frac{1}{2}\sum_{j=1}^{n} \mathbb{I}^1 \otimes \ldots \mathbb{I}^{j-1} \otimes \hat{\sigma}_i^j \otimes \mathbb{I}^{j+1} \otimes \ldots \mathbb{I}^n,$$

where $n = 2s$.

(5) Apply the VQE method with the cost function

$$c(\boldsymbol{\alpha}) = \frac{a}{\max |\lambda_i|^2} \langle \psi(\boldsymbol{\alpha}) | \hat{C}^\dagger \hat{C} | \psi(\boldsymbol{\alpha}) \rangle + b\left(1 - \frac{\langle \hat{\vec{S}}^2 \rangle}{s(s+1)}\right),$$

where $a + b = 1$, and $a, b \in (0, 1)$ (e.g., $a = \frac{1}{2} = b$).

(6) Explore degeneracy of the kernel space by either adding terms $|\langle \psi_i | \psi(\boldsymbol{\alpha}) \rangle|$ to the cost function or by applying the Gram-Schmidt procedure.

(7) Study the large s limit to recover results for the flat (affine) phase space.

The procedure utilizes compactification of the system's phase space for the purpose of making its Hilbert space finite. The dimension of the Hilbert space is controlled by a single parameter s, which labels irreducible representations of the $SU(2)$ group. The flat phase space case is recovered in the large spin s limit. In the article, the procedure has been tested on the example of the de Sitter cosmological model, which has a single classical degree of freedom (the scale factor) and, consequently, a two-dimensional phase space. In the quantum case, kinematics is described by the spin operator $\hat{\vec{S}}$. The quantum constraint of the system has been expressed in terms of the qubits of the quantum register for an arbitrary spin s. This allowed us to apply the VQE method to extract physical states of the model under consideration.

As an example, the procedure has been executed for $s = 1$ and $s = 2$. In the case of $s = 1$, the quantum circuits were evaluated on both a simulator of the quantum computer and the superconducting quantum computer Yorktown. In the case $s = 2$, computations have been performed on a simulator only due to high quantum errors. Both the cases of nondegenerate and degenerate kernels were explored, confirming the correctness of the method.

It has been emphasized that the introduced method does not provide an advantage over classical computations for the case with a single degree of freedom (e.g., homogeneous and isotropic cosmology). However, the advantage is expected while a large number of quantum-gravitational degrees of freedom are considered. Investigation of such a case will be a subject of our further studies.

ACKNOWLEDGMENTS

The research has been supported by the Sonata Bis Grant No. DEC-2017/26/E/ST2/00763 of the National Science Centre Poland. This research was funded by the Priority Research Area Digiworld under the program Excellence Initiative—Research University at the Jagiellonian University in Kraków. Furthermore, this publication was made possible through the support of the ID No. 61466 grant from the John Templeton Foundation, as part of the "The Quantum Information Structure of Spacetime (QISS)" Project (qiss.fr). The opinions expressed in this publication are those of the authors and do not necessarily reflect the views of the John Templeton Foundation.

APPENDIX: RYCZ *ANSATZ*

RYCZ *Ansatz* consists of R_y (RY)

$$R_y(\theta) = \exp\left(-i\frac{\theta}{2}\sigma_y\right) = \begin{pmatrix} \cos\frac{\theta}{2} & -\sin\frac{\theta}{2} \\ \sin\frac{\theta}{2} & \cos\frac{\theta}{2} \end{pmatrix}, \tag{A1}$$

and controlled-σ_z (CZ) gates.

We apply gates $R_y(\theta_i)$, parametrized by different parameters θ_i, on every qubit, and then we apply CZ gates on all pairs of qubits (Fig. 16) or only on some pairs (Fig. 17). This block of gates can be repeated many times (Fig. 18).

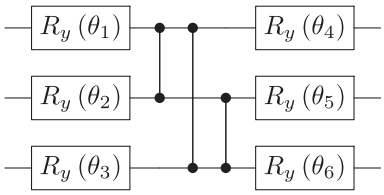

FIG. 16. Quantum circuit for the RY *Ansatz* with full entanglement, and depth = 1.

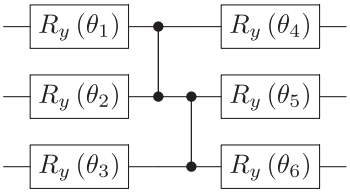

FIG. 17. Quantum circuit for the RY *Ansatz* with linear entanglement, and depth = 1.

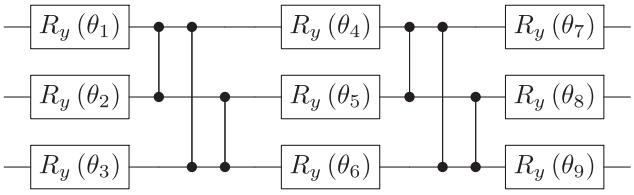

FIG. 18. Quantum circuit for the RY *Ansatz* with full entanglement, and depth = 2.

This *Ansatz* generates states with real coefficients, but since $\hat{C}$ is self-adjoint, we can always choose the eigenvectors to be real. Let $|v\rangle$ be an eigenvector with complex coefficients for the λ eigenvalue (which is real),

$$\hat{C}|v\rangle = \lambda|v\rangle. \tag{A2}$$

Then $|\bar{v}\rangle = |v\rangle^*$ is also an eigenvector for the same eigenvalue,

$$\hat{C}|\bar{v}\rangle = \lambda|\bar{v}\rangle. \tag{A3}$$

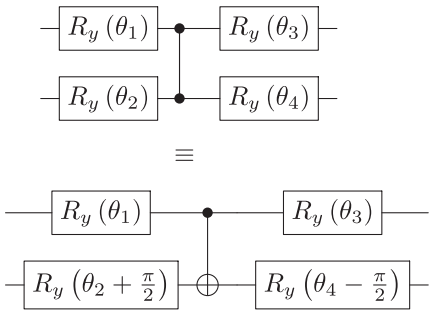

FIG. 19. Quantum circuit for the RYCZ *Ansatz*.

As a consequence, we can take a linear combination of these vectors,

$$|a\rangle = \frac{1}{2}(|v\rangle + |\bar{v}\rangle), \tag{A4}$$

$$|b\rangle = \frac{1}{2i}(|v\rangle - |\bar{v}\rangle), \tag{A5}$$

which are real eigenvectors with eigenvalue λ.

[1] H. Nicolai, K. Peeters, and M. Zamaklar, Classical Quantum Gravity **22**, R193 (2005).
[2] A. Ashtekar and J. Lewandowski, Classical Quantum Gravity **21**, R53 (2004).
[3] J. B. Hartle and S. W. Hawking, Phys. Rev. D **28**, 2960 (1983).
[4] A. Vilenkin, Phys. Rev. D **30**, 509 (1984).
[5] J. Kowalski-Glikman and K. A. Meissner, Phys. Lett. B **376**, 48 (1996).
[6] J. C. Feng, Phys. Rev. D **98**, 026024 (2018).
[7] A. Ashtekar, J. Lewandowski, D. Marolf, J. Mourao, and T. Thiemann, J. Math. Phys. (N.Y.) **36**, 6456 (1995).
[8] T. Thiemann, Classical Quantum Gravity **23**, 1163 (2006).
[9] P. Dzierzak, P. Malkiewicz, and W. Piechocki, Phys. Rev. D **80**, 104001 (2009).
[10] J. Mielczarek and W. Piechocki, Classical Quantum Gravity **29**, 065022 (2012).
[11] J. Mielczarek, Front. Astron. Space Sci. **8**, 95 (2021).
[12] A. Peruzzo, J. McClean, P. Shadbolt, M.-H. Yung, X.-Q. Zhou, P. J. Love, A. Aspuru-Guzik, and J. L. O'Brien, Nat. Commun. **5**, 4213 (2014).
[13] A. Kandala, A. Mezzacapo, K. Temme, M. Takita, M. Brink, J. M. Chow, and J. M. Gambetta, Nature (London) **549**, 242 (2017).
[14] Y. Cao *et al.*, Chem. Rev. **119**, 10856 (2019).
[15] https://pennylane.ai/.
[16] https://qiskit.org/.
[17] https://quantum-computing.ibm.com/.
[18] A. Joseph, J. P. Varela, M. P. Watts, T. White, Y. Feng, M. Hassan, and M. McGuigan, arXiv:2105.13849.
[19] J. Mielczarek and T. Trześniewski, Phys. Lett. B **759**, 424 (2016).
[20] J. Mielczarek, Universe **3**, 29 (2017).
[21] J. Mielczarek and T. Trześniewski, Phys. Rev. D **96**, 043522 (2017).
[22] J. Bilski, S. Brahma, A. Marcianò, and J. Mielczarek, Int. J. Mod. Phys. D **28**, 1950020 (2019).
[23] N. Bao, S. M. Carroll, and A. Singh, Int. J. Mod. Phys. D **26**, 1743013 (2017).
[24] C. Rovelli and F. Vidotto, Phys. Rev. D **91**, 084037 (2015).
[25] D. Berenstein, R. Brower, and H. Kawai, arXiv:2201.02412.
[26] D. Artigas, J. Mielczarek, and C. Rovelli, Phys. Rev. D **100**, 043533 (2019).
[27] D. Artigas, J. Bilski, S. Crowe, J. Mielczarek, and T. Trześniewski, Phys. Rev. D **102**, 125029 (2020).
[28] D. Artigas, S. Crowe, and J. Mielczarek, Classical Quantum Gravity **38**, 085007 (2021).
[29] J. Mielczarek, Universe **5**, 179 (2019).
[30] M. J. D. Powell, A direct search optimization method that models the objective and constraint functions by linear interpolation, *Advances in Optimization and Numerical Analysis*, edited by S. Gomez and J-P Hennart (Kluwer Academic, Dordrecht, 1994), pp. 51–67.
[31] D. Kingma and J. Ba, *Published as a conference paper at the 3rd International Conference for Learning Representations* (San Diego, 2015), arXiv:1412.6980.
[32] M. Schuld, V. Bergholm, C. Gogolin, J. Izaac, and N. Killoran, Phys. Rev. A **99**, 032331 (2019).